Detection of atmospheric rotation by means of the DWD weather radar network

Thomas Hengstebeck[1], Dirk Heizenreder[1] and Paul Joe[2]

[1]*Deutscher Wetterdienst, Frankfurter Str. 135, 63067 Offenbach am Main, Germany*
[2]*Environment Canada, 4905 Dufferin St, Toronto, Ontario M3H 5T4, Canada*

(Dated: 18 July 2014)

1 Introduction

The German Weather Service (Deutscher Wetterdienst, DWD) operates a network of 17 radar stations delivering radar scan data in five minute intervals (see figure 1). Besides the single-sweep terrain-following precipitation scan designed to catch close to ground precipitation, a so-called volume scan is repeatedly taken every 5 min. This scan is comprised of 10 sweeps with elevation angles extending from 0.5° to 25° (cf. figure 2). The lowermost 7 sweeps are taken in the so-called dual-PRF mode in order to combine a large unambiguous range (180 km) with a sufficient measurement interval of radial velocities (extended Nyquist interval -32 to +32 m/s). In the pre-processing procedure, which is performed at the radar site itself (within the radar device's signal processor), a first quality control is achieved by means of a set of filters and thresholds (e.g. Doppler Filter for removing stationary clutter, for basic information see (Seltmann 2000). This pre-processed data is called basic data.

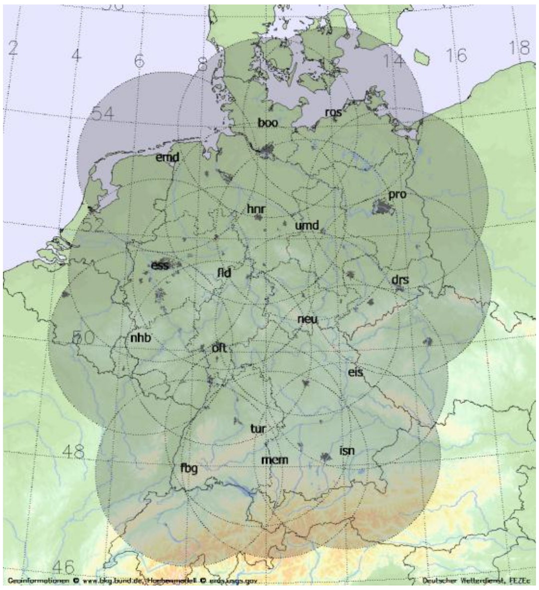

Figure 1: The German radar network: 17 operational C-band weather radar systems completely cover the region of Germany. The map shows the modernized dual-polarimetric radar network as planned for 2015. The dashed lines correspond to the maximum range of the lowermost sweep in the volume scan, which is 180 km.

The basic data from all German radar stations are gathered at the DWD central office in Offenbach am Main in real-time by means of an automated file distribution system (AFD) and are available for follow-up applications. In order to adequately exploit the possibilities of the polarimetric data of the new radar sites, a software framework called POLARA (Polarimetric Radar Algorithms) has been developed (Rathmann and Mott 2012), which also hosts "classical", non-polarimetric algorithms, the mesocyclone detection being one of these. POLARA contains various modules like quality control algorithms, a hydrometeor classification and an improved quantitative precipitation estimation, so that there is the possibility of synergetic exchanges. As part of the quality control the correction of dual-PRF unfolding errors has been improved to eliminate spurious high shear regions and restore corrupted real mesocyclone vortices, an essential prerequisite for the follow-up mesocyclone detection algorithm. The radar basic data as well as all products are visualized in the meteorological workstation system NinJo where a so-called SCIT-Layer (Storm Cell Identification and Tracking) optionally shows the mesocyclone detections within the NinJo meteorological workstation system (Joe, Koppert, et al. 2005).

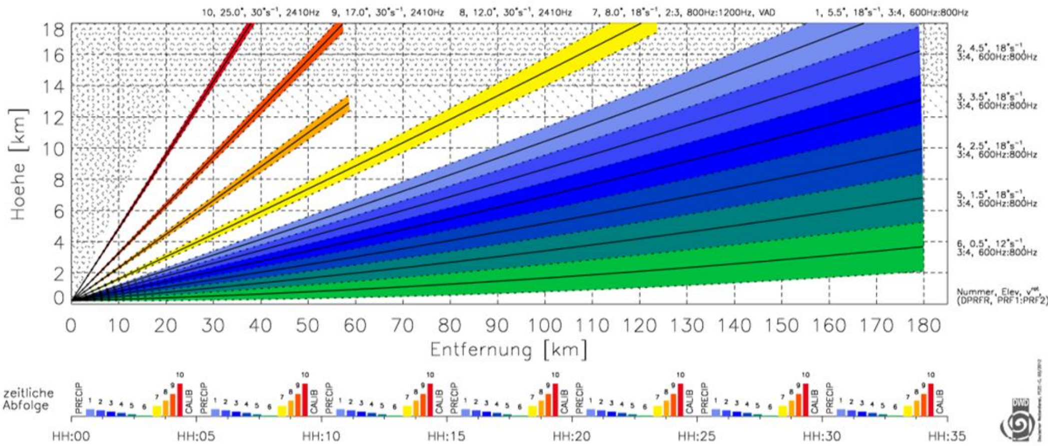

Figure 2: The volume scan strategy of DWD: The scan pattern comprises 10 sweeps with elevation angles from 0.5° to 25° and is repeated every 5 minutes supplying reflectivity and radial velocity as well as dual-polarimetric moments. A dual PRF unfolding error correction is applied to the radial velocity data of the 7 lowermost sweeps giving a sound basis e.g. for shear calculations in follow-up algorithms.

The scan strategy as described above offers a scanning of the troposphere with comparably high spatial and temporal resolution, so that small-scale, dynamic severe weather phenomena can be captured. A mesocyclone – defined as a vortex of rotating air within a thunderstorm (see figure 3) – is such a dynamic feature. Mesocyclones are frequently found as rotating updrafts in supercells and often occur in connection with severe weather events like heavy rain, hail, strong surface winds and tornadoes.

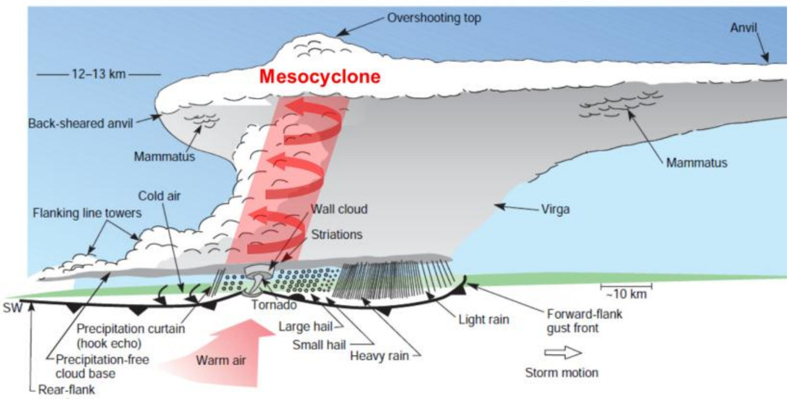

Figure 3: Sketch of a classical supercell, the rotating updraft (mesocyclone) is indicated as red shaded area, adopted from (Wallace and Hobbs 2005)*. Mesovortices also occur in other convective systems, e.g. MCS with bow echo structure.*

Therefore, the detection of mesocyclonic shear regions in Doppler radar data gives valuable information for issuing nowcasts and severe weather warnings.

The mesocyclone detection algorithm at DWD uses a pattern vector approach to identify the regions of high shear within the center of mesocyclonic rotation and provides 3D mesocyclone objects. A unique aspect of the DWD algorithm is the merging of 2D mesocyclone features from multiple network radars in overlapping regions to create a single 3D detection. The mesocyclone objects are validated using secondary features such as VIL. A severity metric is created using mesocyclone object properties (shear, momentum) and the secondary features and the various mesocyclone objects are then ranked and issued to the forecaster as guidance by means of the NinJo meteorological workstation system.

Meteorologists can judge the significance of mesocyclone detections using the severity scale as guidance and applying persistency and consistency checks (track of mesocyclone detections, additional occurrence of typical weather features e.g. hook echoes). A further means to validate a mesocyclonic rotation is given by the rotation and rotation-track products (see section 4).

2 Quality Assurance of Doppler Wind data

The essential input for the mesocyclone detection and the rotation products is comprised of the Doppler scan data. This scan, as introduced above, is configured in such a way as to achieve both an adequate unambiguous Doppler velocity interval and a suitable maximum range. The dual-PRF scan with 800/600 Hz permits a measurement of radial velocities within -32 to +32 m/s (32 m/s is the Nyquist velocity V_{Nyq}). The maximum range is determined by the high PRF (800 Hz) and amounts to 180 km, which ensures a complete coverage of Germany with the 17 radar stations of DWD.

Unfortunately the dual PRF unfolding technique relies on the assumption, that adjacent range-bins show the same true radial velocity within a tolerance of 2.65 m/s (for the 800/600 Hz mode taking into account a radar wavelength of 5.3 cm). This tolerance can be exceeded due to ubiquitous noise fluctuations on top of the true velocity values and appear as randomly scattered points. In high shear regions, the tolerance can be exceeded due to the real shear. 'The distribution of these velocity errors is discrete, as the errors are multiples of twice $V_{Nyq,800}$ or $V_{Nyq,600}$. In practice this most commonly results in errors of +/-V_{Nyq}' (citation from (May 2000) with adapted PRFs). These quality errors are not removed by the on-site pre-processing quality assurance.

However, the dual PRF unfolding errors are corrected by means of a detection-correction filtering algorithm. Within the POLARA quality assurance module (Werner 2014) a Laplacian operator technique based on (Joe and May 2003) is used. This method applies a 'discrete filtering' taking into account the affected range-bin's PRF, which counteracts an over-smoothing (see figure 4 and figure 5). The Laplace Filter basically uses a pixel window to calculate a correction value for the central pixel. The dual-PRF correction in POLARA has been extended towards a 2-stage process where a large window is used to identify spurious pixels to be excluded from calculations within a small window correction process.

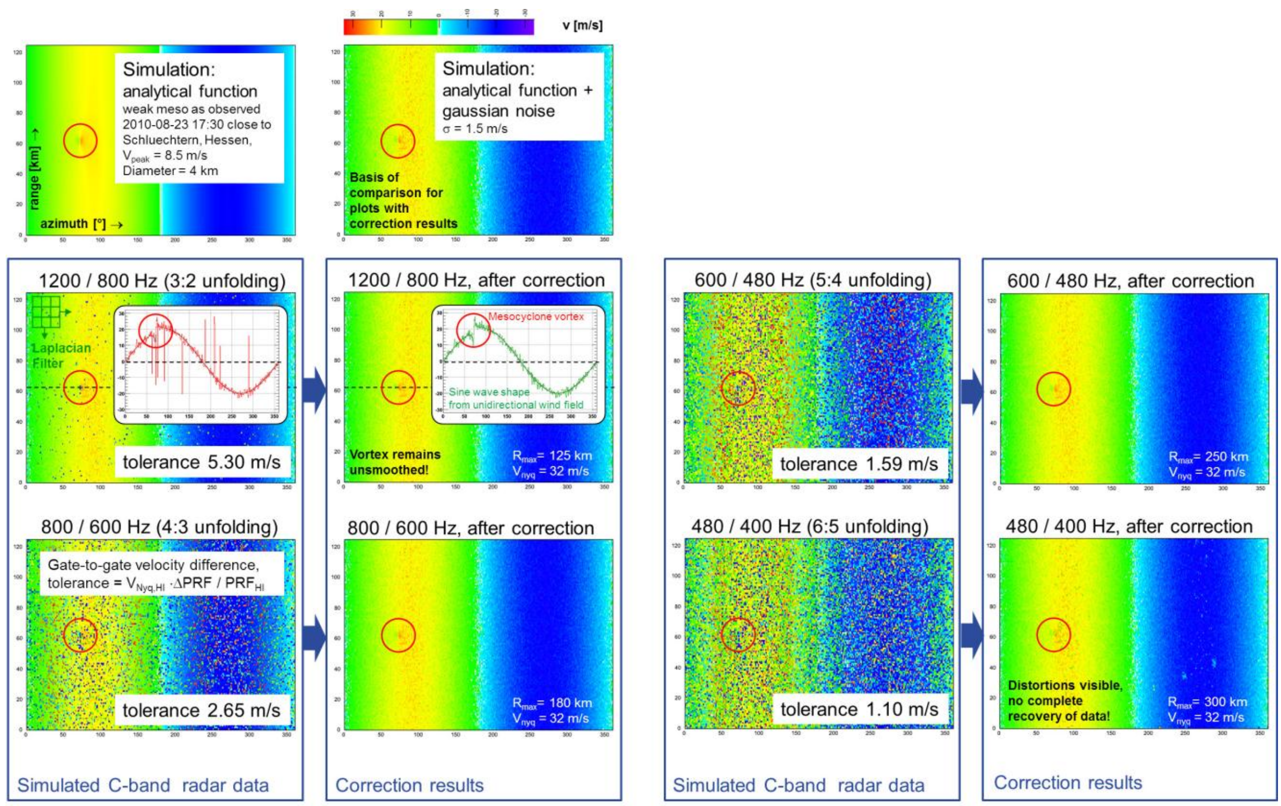

Figure 4: Series of simulations showing the performance of the dual-PRF unfolding error correction for different PRF settings.

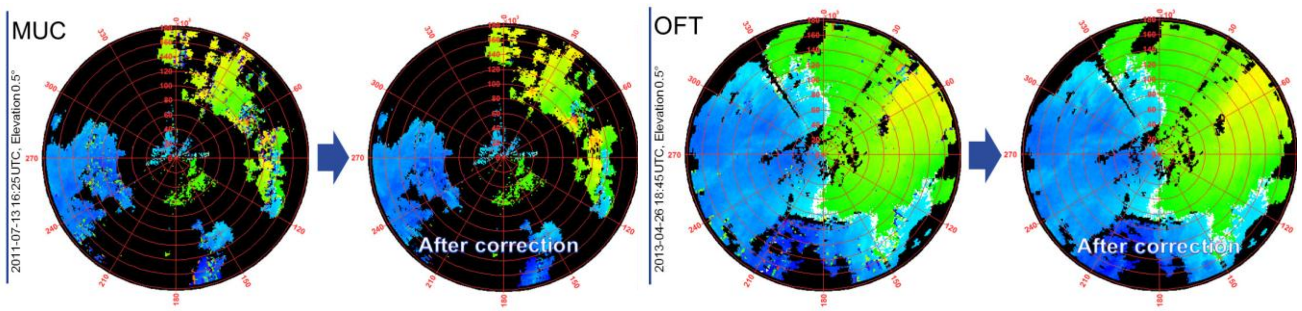

Figure 5: Observational data without and with dual-PRF unfolding error correction. The old radar system at the Munich site (MUC) with a test scan setup of 600 / 800 Hz dual-PRF mode has been chosen in order to demonstrate a "worst case scenario". The site Offenthal (OFT) close to Frankfurt is equipped with a modern radar system.

3 The mesocyclone detection algorithm

As outlined in the last section the Doppler data are quality controlled by means of a filtering algorithm which mitigates the occurrence of dual-PRF unfolding errors, which otherwise would lead to spurious values of azimuthal shear.

The next step is the calculation of the azimuthal shear for each sweep of the Doppler volume. Here, insignificant shear values < 2 m/s (adapted to the data's noise level) are set to 'missing value'. It should be noted that the mesocyclone detection in its current configuration performs a search for cyclonic rotation, which is the dominant 'mode' of mesocyclonic rotation on the earth's northern hemisphere. Cyclonic rotation corresponds to positive values of azimuthal shear (the radial velocity is increasing in direction of increasing azimuth). Treating negative shear as noise reduces the influence of remaining dual PRF unfolding errors in regions of positive, cyclonic shear since dual PRF unfolding errors are often associated with a change of sign in the spurious velocity estimate.

The mesocyclone detection can be divided into three main parts, each of which is based on the precursor part: The detection of pattern vectors, the grouping of pattern vectors to features and, finally, the combination of features to 3D-mesocyclone objects. The mesocyclone detection approach basically follows (Zrnic, Burgess and Hennington 1985).

A pattern vector is a sequence of positive azimuthal shear at constant range. Figure 6 left shows a Doppler rotation signature (typical dipole) and the series of pattern vectors that can ideally be found within the area of rotation. The pattern vector search accepts interruptions of one range-bin within a pattern vector. Each pattern vector is filtered with respect to Doppler angular momentum and shear. The Doppler angular momentum is a specific or relative physical quantity since the air mass is unknown. First, low thresholds t_{low} must be passed (momentum > $t_{low,\ momentum}$ and shear > $t_{low,shear}$), so that only shear regions above noise threshold are accepted for further analysis. Second, high shear and momentum thresholds are applied (moment > $t_{high,\ momentum}$ or shear > $t_{high,shear}$). Here, the idea is to pick up high shear, small-scale rotations (late, mature stage of mesocyclone development) as well as high momentum, large scale rotations (early stage of mesocyclone development).

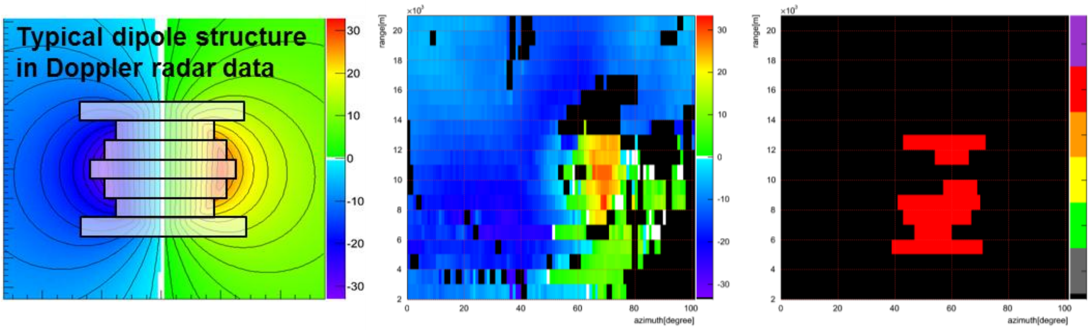

Figure 6: Left: Typical mesocyclone vortex as it appears in Doppler radar velocity data (here assumed: distance to radar much larger than Mesocyclone diameter, infinite resolution of radar). Pattern vectors are indicated as transparent white boxes. The wind field can be described by the Rankine Combined Vortex Model and consists of an inner part (rigid rotation) and an outer part where the vortex wind field is embedded into the environmental wind field. The group of pattern vectors resembles a feature. Middle: quality controlled radial velocity data recorded at radar site Dresden on May 24th 2010 during the occurrence of a tornadic supercell. Right: the corresponding detected pattern vectors. The red color indicates that - after combining all features detected at this region - a mesocyclone with severity level 4 was found.

The mesocyclone detection proceeds by grouping the pattern vectors to features. In the ideal case, a feature corresponds to a complete rotation signature within a sweep and is build up by several pattern vectors adjacent in range. However, in reality, there is always some noise present (remaining dual PRF unfolding errors, missing data due to signal filters). Thus, the following criteria are used to extract only meaningful features and, at the same time, allow for imperfect data:

- First, the number of detected pattern vectors must exceed a certain threshold that depends on the range resolution as well as on the minimum assumed vortex spatial extent (currently set to 3, the range resolution is 1 km).
- Second, symmetry criteria (spatial extension of feature should be roughly equal in azimuth and range direction) must be passed (gaps of one range bin between pattern vectors are allowed).

Finally, the Doppler volume with its sweeps and related features (2D-objects within a sweep) are combined to three-dimensional, vertically aligned mesocyclone objects (cf. figure 7).

Figure 7: Left: Scheme showing a 3D mesocyclone object consisting of three features that are detected in 3 consecutive sweeps. Right: In case of detections from multiple radar sites (overlapping scan regions) the geo-referenced features are merged into the same mesocyclone object (no multiple detections of the same mesocyclone).

The condition of vertical alignment (overlap) between two features is fulfilled if the offset of the feature centres is less than the sum of the features radii. For each detected mesocyclone object, maximum and mean shear, maximum and mean momentum as well as the properties shown in table 1 are calculated taking also into account the reflectivity information from the Doppler volume.

TABLE 1: Thresholds for severity calculation (connected by logical AND).

Mesocyclone cell attributes		**Severity-Level**				
		1	**2**	**3**	**4**	**5**
Max. reflectivity [dBZ]	≥	10	30	40	50	55
Avg. Reflectivity [dBZ]	≥	10	20	25	35	40
Height above ground [km]	≤	5	3	2.5	2	1.5
Meso-Height [km]	>	0	0	2	4	6
VIL [kg m^{-2}]	>	2	5	10	20	30
Echo top height [km]	>	1	3	4	5	7
VIL density [g cm^{-3}]	>	0	1	1.5	2	2.5
Max. shear [m/s / km]	>	0	0	0	15	20
Max. momentum [m/s · km]	>	0	0	0	150	200

A definition of VIL and VIL density can be found in (Greene and Clark 1972) and (Graham and Struthwolf 1999). In the latter publication cell-based VIL, which is used for the MDA, is described in some detail. As a last step, a severity ranking is computed. Table 1 shows the current set of thresholds used for severity calculation. Properties of the region of the detected mesocyclonic rotation like mean / maximum reflectivity, cell-based VIL (vertically integrated liquid water), VIL density, height of lowermost detected rotation signature over ground, total height of rotational column and echo top height are calculated. The severity ranking validation is to a great extent done with the help of the reflectivity data. However, ongoing tests with an alternative severity scale putting less emphasize on reflectivity related attributes and more on shear and depth of rotation show promising results.

The severity levels 2-5 imply mesocyclonic rotation with increasing strength and clearness. Severity-level 1 rather serves for test / tuning purposes, but may also give hints to early stages of rotation. The latitude-longitude coordinate-pair of the mesocyclone-cell is determined as shear weighted mean of the lowest 3 km of the mesocyclone object. Some of the mesocyclone attributes, in particular VIL, are affected by the geometrical resolution, which naturally changes with the distance from the radar. Therefore a fuzzy logic scheme is used, which allows a slight violation of the thresholds. This means that e.g. VIL may drop by as much as 4.5% below the threshold of the current severity class without a change of the severity (adjustable value).

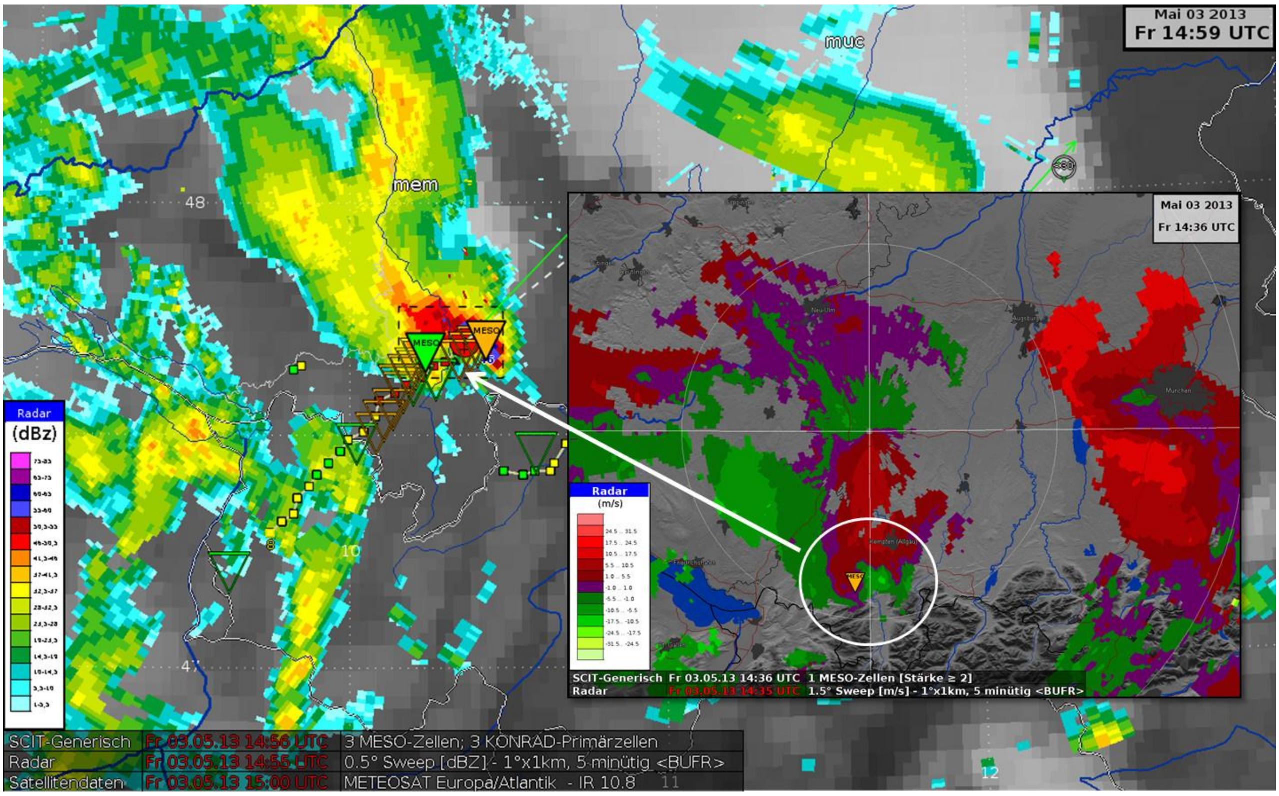

Figure 8: Example of mesocyclone detections visualised by means of the NinJo workstation system at DWD. Solid triangles denote current mesocyclone detections (system time given in label in upper right corner), open triangles denote historic mesocyclone detections. The small rectangles show historic KONRAD cell detections (Lang, et al. 2003). The embedded graphic shows the Doppler wind data for 14:35 UTC. The cyclonic signature is clearly visible. This weather case is addressed in the next section as well.

4 The rotation and rotation track algorithms

The rotation algorithm was introduced at DWD as a supplement to the mesocyclone detection and is meant for visualizing the azimuthal shear connected with rotation in meso-(anti)cyclones. It is inspired by the NSSL LLSD and rotation track algorithms (Smith and Elmore 2004).

In the DWD version rotational shear is calculated from the dual-PRF unfolding error corrected (pre-processed) radial velocity volume sweep data after application of a smoothing 3×3 pixel window filter. Naturally, shear values as derivatives of the radial velocity field are noisy with fluctuations especially influencing the vicinity of a radar site. It was found that a further averaging procedure can effectively mitigate this noise. The averaging is performed in vertical direction, so that in addition to the noise suppression an amplification of deep rotation is obtained (rotation in column, compare also figure 3).

The POLARA rotation algorithm starts by generating a 0°-elevation sweep. Each pixel within this sweep is assigned a value corresponding to the average azimuthal shear in the vertical column above the pixel. For the low level (LL) rotation product the column extends from 0 to 3 km above ground level (AGL). In case of the mid-level (ML) rotation product the column is ranging from 3 to 6 km height AGL. A minimum reflectivity of 5 dBZ is necessary for a shear value to enter the averaging procedure. Both LL and ML rotation products show positive (cyclonic) and negative (anti-cyclonic) shear. The related track products are obtained by pixel-wise accumulating the maxima from the LL and ML rotation products of the last 3 hours (which corresponds to 36 sweep products due to the 5 min scan strategy), so that only positive shear is picked up.

For both rotation and rotation track products, which are related to a radar site, composite products are generated. In case of the rotation products (LL and ML), in regions of overlapping radar scans the shear value is taken, the absolute value of which is largest. In case of the track products only positive azimuthal shear is evaluated. The more frequently occurring cyclonic vortices are represented by an area of positive shear (center of rotation) flanked on two sides by negative shear values (regions where the rigid rotation of the inner core merges into surrounding wind field). Accumulating both positive and negative shear values (by investigation of absolute value) would result in a complicated picture showing two negative rotation tracks beside each positive rotation track and vice versa.

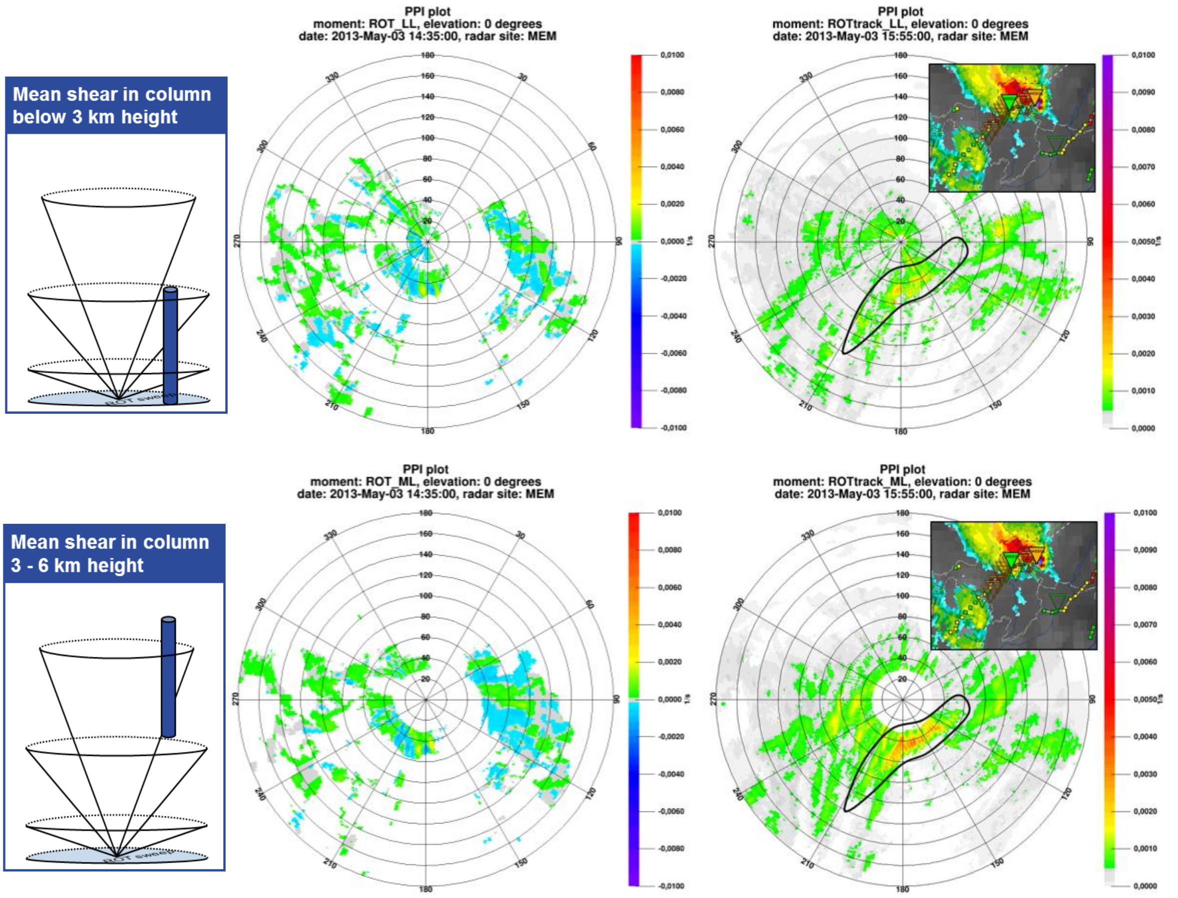

Figure 9: Top Left: low-level rotation (ROT-LL) value calculation for a single pixel of the polar "ROT" sweep coordinate grid. Top middle: ROT-LL sweep from observational data (see image label for details). Two distinct "yellow spots" of positive shear are visible ca. 50 km from the radar center in southern direction (180 ° azimuth). Top Right: ROT-LL Track (time interval for accumulation is 3 hours). In this weather case, the rotation is more restricted to higher atmospheric layers as can be seen from the ROT-ML product. Bottom Left: mid-level rotation (ROT-ML) value calculation for a single pixel of the polar "ROT" sweep coordinate grid. Bottom Middle: ROT-ML sweep from observational data (see figure label for details). Also here two distinct regions of positive shear can be seen. Bottom Right: ROT-ML Track (time interval for accumulation is 3 hours). The embedded NinJo screenshot shows the mesocyclone and cell detections for comparison (see also figure 8).

Rotation and rotation track products should be used in addition to the mesocyclone detection as verification check. Moving rotating cells are expected to produce tracks of high azimuthal shear visible in the rotation track product. The low level and mid-level rotation track products can help to distinguish between close to ground (implication for possible occurrence of tornadoes) and mid-level atmospheric rotation.

A discussion of non-mesocyclonic signatures can be found in (Miller, Lakshmanan and Smith 2012). Here, it is stated that "significant vertical shear near the surface can cause false high azimuthal shear values very close to the radar" (Miller, Lakshmanan and Smith 2012, 577) and that "bands of high azimuthal shear values associated with linear meteorological phenomena like outflow boundaries and bow echoes also appear in the rotation track fields" (Miller, Lakshmanan and Smith 2012, 580). However, such signatures can usually be distinguished by eye from real rotation tracks.

5 Current status and future developments

The mesocyclone detection with preceding quality assurance has been running in operational mode at DWD since 2011. The visualization of detected mesocyclones is available based on the severe weather forecasting tools in NinJo (Joe et al., 2005) to provide guidance for forecasters at the central and regional weather forecast offices of DWD. A re-implementation within the POLARA software framework was accomplished in 2012. Here, the quality assurance has been extended towards a 2-stage process (see section 3) and the merging of 2D mesocyclone features from multiple network radars in overlapping regions was introduced. The rotation and rotation-track products are produced in real time but are not yet available for forecasters; a validation still has to be done before the integration in NinJo will be finished.

DWD plans to integrate the results of the mesocyclone detection into the NowCastMIX system (James, et al. 2013).

Further developments in POLARA will include a 3D-cell detection and tracking. Dual polarimetric algorithms within POLARA already provide test products for verification studies (e.g. hydrometeor classification, see (Steinert 2014)). A big advantage of a common software framework is that the implemented algorithms can benefit from each other by directly exchanging data. For example, the information from a 3D-cell detection, from the mesocyclone detection and from a hydrometeor classification (presence of hail) can be put together to have a distinguished picture of a storm cell. Lifetime studies may be feasible.

Acknowledgement

The support offered by Patrick Tracksdorf, Nils Rathmann, Michael Mott, Dr. Manuel Werner and Jörg Steinert concerning the implementation work in POLARA was greatly appreciated.

References

Graham, R. A., and M. Struthwolf. "VIL Density as a potential hail indicator across northern Utah." *Western Region Technical Attachement No. 99-02*, 1999.

Greene, D. R., and R. A. Clark. "Vertically Integrated Liquid Water - A New Analysis Tool." *Mon. Wea. Rev*, 1972: 548-552.

Hengstebeck, T., D. Heizenreder, P. Joe, and P. Lang. "The mesocyclone detection algorithm of DWD." *6th Europ. Conf. on Severe Storms*, 2011.

James, P., S. Trepte, B. Reichert, and D. Heizenreder. "NowCastMIX - automatic integrated warnings from continuously monitored nowcasting systems based on a fuzzy-logic approach with optimized estimates of storm cell vectors." *7th Europ. Conf. on Severe Storms*, 2013.

Joe, P., and P. T. May. "Correction of Dual PRF Velocity Errors for Operational Doppler Weather Radars." *J. Atmos. Oceanic Technol.*, 2003: 429-442.

Joe, P., et al. "Severe Weather Forecasting Tools in NinJo." *World Weather Research Program Symposium on Nowcasting and Very Short Range Forecasting*, September 5-9, 2005.

Lang, P., O. Plörer, H. Munier, and J. Riedl. "KONRAD - Ein operationelles Verfahren zur Analyse von Gewitterzellen und deren Zugbahnen, basierend auf Wetterradarprodukten." *Berichte des Deutschen Wetterdienstes*, 2003.

May, P. T. "Mesocyclone and Microburst Signatur Distortion with Dual PRT Radars." *J. Atmos. Oceanic Technol.*, 2000: 1229-1233.

Miller, M. L., V. Lakshmanan, and T. Smith. "An Automated Method for Depicting Mesocyclone Paths and Intensities." *Weather and Forecasting*, 2012.

Rathmann, N., and M. Mott. "Effective radar algorithm software development at the DWD." *7th Europ. Conf. On Radar*, 2012.

Seltmann, J. "Clutter versus radar winds." *Phys. Chem. Earth*, 2000: 1173-1178.

Smith, T. M., and K. L. Elmore. "The Use of Radial Velocity Derivatives to Diagnose Rotation and Divergence." *11th Conference on Aviation, Range, and Aerospace Meteorology*, 2004.

Steinert, J. „Hydrometeor Classification for the DWD Weather Radar Network: First Verification Results.“ *8th Europ. Conf. on Radar in Meteorology and Hydrology*, 2014.

Wallace, J. M., and P. V. Hobbs. *Atmospheric Science.* 2005.

Werner, M. „A New Radar Data Post-Processing Quality Control Workflow for the DWD Weather Radar Network.“ *8th Europ. Conf. on Radar in Meteorology and Hydrology*, 2014.

Zrnic, D. S., D. W. Burgess, and L. D. Hennington. "Automatic Detection of Mesocyclonic Shear with Doppler Radar." *J. Atmos. Oceanic Technol.*, 1985: 425-438.